Journal of the Physical Society of Japan
Vol. 55, No. 8, August, 1986, pp. 2648–2652

Localized Electron Heating Experiments by Ion Bernstein Wave in the TNT-A Tokamak

Shunjiro SHINOHARA, Osamu NAITO, Yoshio UEDA,
Hiroshi TOYAMA and Kenro MIYAMOTO

Department of Physics, Faculty of Science,
University of Tokyo, Bunkyo-ku, Tokyo 113

(Received January 27, 1986)

Plasma heating by ion Bernstein wave in the range of $2\omega_D \lesssim \omega \lesssim 3\omega_D$ is investigated in deuterium dominant plasma of the TNT-A tokamak. The localized electron heating is observed at the harmonic ($3\omega_D$) and subharmonic ($2.5\omega_D$) resonance layers, while the electron heating on the whole plasma region is observed at $\omega = 2\omega_D$. It is also shown that the heating is efficient and heating layer is localized by ion Bernstein wave in comparison with fast magnetosonic wave.

Plasma heating by ion Bernstein wave (IBW)[1] at the ion cyclotron harmonic frequency has been anticipated as a promising supplementary heating method in reactor plasmas. Using this wave, waveguide operation, excellent accessibility condition and efficient ion damping even at the higher harmonics can be expected. Although mode conversion from fast magnetosonic wave to ion Bernstein wave was investigated in several tokamaks,[2-6] directly launched ion Bernstein wave heating experiments are a few; the excitation, propagation, and heating by this wave were studied in ACT-1 low temperature toroidal device.[7,8] In the JIPPT-II-U tokamak,[9,10] efficient ion heating was observed at the third harmonic frequency of $^4He^{2+}$ minority ion, and the hydrogen damping at $\omega = 1.5\omega_H$ was suggested (ω_H: proton cyclotron frequency).

Theoretically, the nonlinear ion heating at the cyclotron subharmonic frequency can be also expected by the application of ion Bernstein wave; this ion heating comes from the enhancement of the acceleration due to a particle trapping,[11] and the nonlinear ion cyclotron (Landau) damping due to the self interaction of IBW.[12]

Experimental results on plasma heating at the harmonic and the subharmonic frequencies by IBW are not sufficient, and there are few results on the electron heating profile. In addition to these, few examples are found as to the comparison between the fast magnetosonic wave and ion Bernstein wave heatings in the same machine.

In this letter, plasma heating experiments by IBW are reported in deuterium dominant plasma of the TNT-A tokamak[13,14] in the range of $2\omega_D \lesssim \omega \lesssim 3\omega_D$ (ω_D: deuteron cyclotron frequency). In addition to the third harmonic frequency of the deuteron, localized electron heating profile is first observed at $\omega = 2.5\omega_D$, which can be explained as the ion damping, considering the power deposition profile. (Three dimensional ray tracing calculation has been also made.) The electron heating at the second harmonic frequency, and the comparison of ion Bernstein wave heating with fast magnetosonic wave heating are also presented.

Typical parameters in the TNT-A tokamak experiments are the followings: major radius $R = 40$ cm, minor radius $a = 9$ cm, elongation ratio $\kappa = 1.2$, plasma current $I_p = 3.5$ kA (low current operation to allow probe insertion), loop voltage $V_l = 5.5$–6 V, mean plasma density $\bar{n}_e = 6-8 \times 10^{12}$ cm^{-3}, central electron temperature $T_e(0) \sim 20$ eV, discharge duration time ~ 20 ms, and ratio of total radiated power P_r measured by the bolometer to ohmic power $P_{ohm} \sim 0.9$. (There were no ion temperature measurements.) Deuterium gas is used and the deuteron cyclotron harmonic and subharmonic frequencies are chosen. Though hydrogen gas is not introduced into the vacuum chamber, there remains a little amount of hydrogen on the wall surface; the concentration of the minority proton is estimated to be $\sim 4\%$ from the ratio of H_α to D_α line intensities.

The experimental conditions of ICRF heating system[15] are as follows; the frequency of the generator is 5.6 MHz corresponding to $2\omega_D \lesssim \omega \lesssim 3\omega_D$, i.e., $3.7\,\mathrm{kG} \gtrsim B_t$ (toroidal field) $\gtrsim 2.4$ kG. The pulse width is 4 ms, the input RF power P_{inp} is 3–12 kW and the net RF power P_{net} absorbed by the plasma is 0.5–2 kW. The IBW loop antenna, 1.6 cm wide and 7 cm long, is located on the low field side along the toroidal direction with single screen of poloidal Faraday shield. In order to excite fast magnetosonic wave, the half turn loop antenna, 1.6 cm wide and 38 cm long, with single screen of toroidal Faraday shield is also located on the low field side, and it is 12 cm toroidally away from the IBW antenna. These two antennas are located on nearly the same radial position as the fixed limiter of $a=9$ cm.

The electron temperature profile is obtained with Langmuir probes (single and double probes from the plot of probe current versus probe voltage with good reproducibility. These probes are located near and 180° toroidally away from the antennas. As the measurements are done at $z=5$ cm (distance from the equatorial plane), the obtained values correspond to $\sim 80\%$ of those at $z=0$ cm, assuming the parabolic electron temperature profile. The local heating near the antenna by ion Bernstein wave is not found, as the electron temperature obtained by these probes agrees well each other. By inserting probes (outer diameter of insulating pipe is 0.8 cm) into near the center of the plasma, plasma parameters are affected little with the fixed plasma current of 3.5 kA; V_l increases by $\lesssim 5\%$, changes of soft X-ray emissivity above 150 eV by the surface barrier diode and the mean plasma density are $\lesssim 5\%$. The plasma position is also moved little (<0.5 cm).

Measurements are done near the time of plasma current peak of 10 ms, i.e., 2 ms after the initiation of the RF pulse. Heating effects can be expected as $P_{net}/(P_{ohm}-P_r) \sim 1$. With the IBW heating, plasma current increases by $\sim 5\%$, loop voltage decreases by $\lesssim 5\%$ and plasma density decreases by 5–10%. Changes of soft X-ray emissivity above 150 eV and total radiated power are little ($<5\%$).

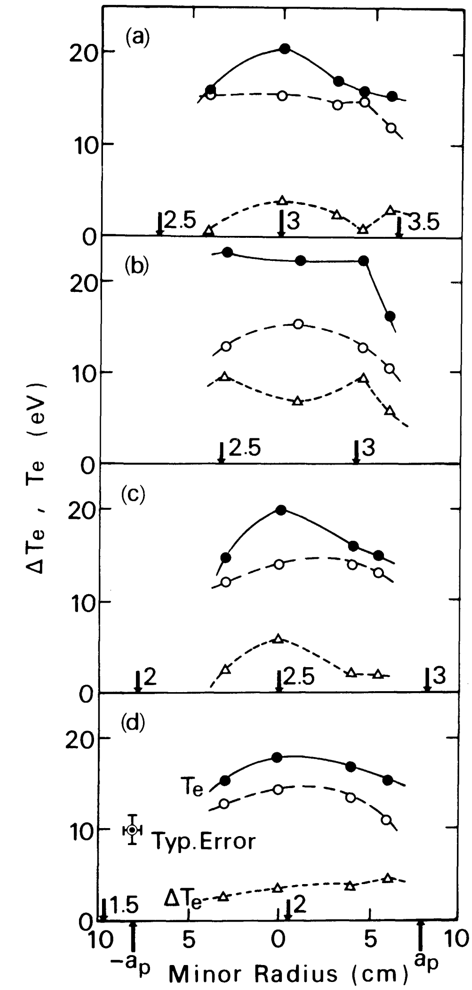

Fig. 1. Radial profiles of electron temperature with (●) and without (○) RF pulse, and increase in electron temperature (△) by ion Bernstein wave. In the case of (a), (b), (c) and (d), toroidal field B_t is 2.44 kG, 2.69 kG, 2.95 kG and 3.70 kG, respectively, and wave frequency f is 5.6 MHz. Positions of harmonic and subharmonic resonance layers, and plasma radius a_p at $z=5$ cm are also shown.

Experimental results on the IBW heating are summarized in Fig. 1. Radial profiles of the electron temperature with and without this wave, and the increase in the electron temperature are shown, varying the toroidal field. (The net RF power is higher in Fig. 1(b) than that in other cases.) The localized electron heating at $\omega=2.5\omega_D$, located on the plasma center, is observed in Fig. 1(c) and is also observed at $\omega=3\omega_D$ in Fig. 1(a). In the case that there are both $2.5\omega_D$ and $3\omega_D$ resonance layers in the plasma, the electron temperature profile is broad (Fig. 1(b)). From these results, the localized heating near the subharmonic ($2.5\omega_D$) and the third harmonic ($3\omega_D$) cyclotron resonance layer is elucidated. Contrary to the above results, the electron temperature profile is broad and the whole plasma region is heated when the second harmonic resonance layer is located near the plasma center (Fig. 1(d)).

The antenna field error and/or the reproducibility of the IBW heating is examined. The IBW antenna can be rotated (the axis of the rotation is at the feedthrough part) so as to excite the opposite (toroidal direction) antenna current. There is no appreciable difference between the data with the rotation and that without one, which can neglect the field error even if it exists and shows the reproducibility of this heating.

Next, the difference of the electron temperature profile between ion Bernstein wave heating and fast magnetosonic wave heating is investigated. Figure 2 shows the electron heating effects at $\omega=3\omega_D$ by both waves. It is clear that the heating layer is localized at

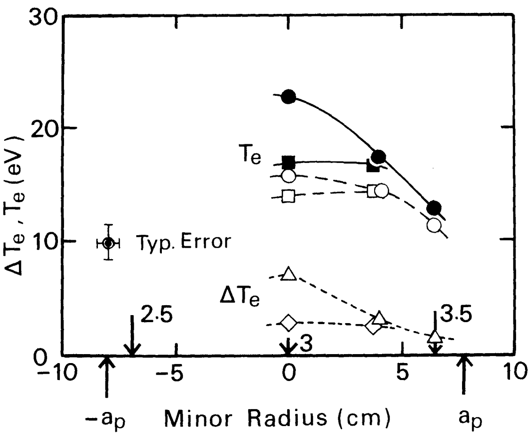

Fig. 2. Electron heating effects with ion Bernstein wave (with (●) and without (○) RF pulse) in comparison to fast magnetosonic wave (with (■) and without (□) RF pulse) in the case of $B_t=2.44$ kG and $f=5.6$ MHz. The triangle (△) and lozenge (◇) denote increase in electron temperature by ion Bernstein wave and fast magnetosonic wave, respectively. Positions of resonance layer and plasma radius are also shown.

the third harmonic resonance layer and the heating efficiency is better in the IBW case. In the second harmonic case, the electron heating efficiency is also several times higher by ion Bernstein wave than that by fast magnetosonic wave.

The cause of the observed electron heating by IBW is considered. There are three possible reasons for this heating; the direct electron heating due to the electron Landau damping, the power flow to the electron from the deuteron, which is heated by the wave, through the collision between them, and the collisional damping with the neutral particles.

First, three dimensional ray tracing calculation has been made in order to estimate the electron Landau damping, using the same code in ref. 16. Figure 3 shows the wave power and the electron power deposition profile in the case that $\omega=3\omega_D$ is located on the plasma center. At low parallel refractive index n_z ($n_z=21.3$ and 42.6, i.e., toroidal mode number $n=1$ and 2), the wave power is absorbed at $\omega=3\omega_D$. As n_z increases, the wave power absorption by the electron Landau damping becomes dominant and this damping region approaches the plasma surface. The excited n_z spectrum is broad ($n_z \lesssim 300$) determined from the antenna configuration, and if the power absorption by the electron Landau damping dominates that by the cyclotron harmonic damping, the expected electron temperature profile becomes broad. The same features must be obtained at $\omega=2.5\omega_D$ damping (Except for the case of $n_z\sim 65$, central electron heating does not occur). The expected electron temperature profile by the calculation is different from the experimental one. Therefore, the direct electron Landau damping can be excluded as a candidate of the main electron temperature rise at $\omega=2.5\omega_D$ and $3\omega_D$.

Second, the power flow from the deuteron to the electron is considered. The energy confinement time of the electron and the deuteron, and the thermal relaxation time between these two species are estimated to be ~ 1 ms, $\gtrsim 1$ ms and ~ 0.2 ms, respectively. Using these values, the mean temperature rise of the electron and the deuteron by the wave is expected to be 3–6 eV/kW, which is consistent

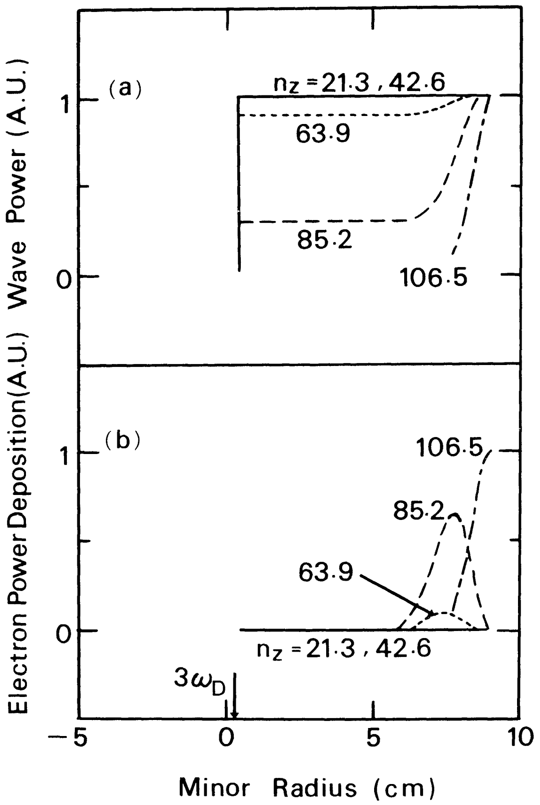

Fig. 3. Three dimensional ray tracing calculation of wave power profile and electron power deposition profile for different initial values of parallel refractive index n_z with TNT-A parameters. Here, $n_z=21.3$ corresponds to the toroidal mode number $n=1$ and the parallel wave number $k_z=2.5\ \mathrm{m}^{-1}$.

with the measurements.

Third, the collisional damping with the neutrals is calculated using the same code in ref. 17. This damping region is not at the central plasma part, but at least at the outer part of the two thirds of the plasma radius, which is not consistent with the experimental results.

Experimental results that antenna loading resistance at low n_z is larger than that at high n_z also support the above conclusion, i.e., the main electron heating is not due to the electron landau damping and the collisional damping. In the TNT-A tokamak, there is a tendency that the electron temperature increases with the decrease in the plasma density. As the electron temperature is expected to rise only by $\sim 5\%$ from the decrease in the plasma density by 5–10%, the effect of the plasma density on the electron heating is small. The effect of the proton on the electron heating is also neglected because of the small concentration of $\sim 5\%$.

From these considerations of the electron heating mechanism, the main rise of the electron temperature can be explained as the result of the direct deuteron heating.

As for the nonlinear ion damping at $\omega=2.5\omega_D$, the threshold of the power governing the nonlinear absorption in TNT-A device is ~ 0.1 kW from the calculation of eq. (12) in ref. 12, which is an order of magnitude smaller than that in the experiments. According to ref. 11, the nonlinear absorption occurs if the value of α (ratio of $E\times B$ drift velocity to perpendicular phase velocity) exceeds ~ 0.2. It is estimated that the experimental value is the same order of the threshold of α. The other candidate of the heating mechanism at $\omega=2.5\omega_D$ is the fifth harmonic heating of D_2^+ or not fully ionized ions of O^{4+} and C^{3+} in the case of $T_e(0)\sim 20$ eV. In this occasion, the effect of the proton can be neglected because of no harmonic and subharmonic resonances of this ion. In any case, the localized electron heating, interpreted as the power flow from the deuteron heated as the result of the ion damping at $\omega=2.5\omega_D$, is obtained.

In conclusion, ion Bernstein wave heating experiments have been done in deuterium dominant plasma of the TNT-A tokamak. The first observed localized electron heating (the electron temperature increases by $\sim 30\%$) at $\omega=3\omega_D$ and $2.5\omega_D$ can be explained as the ion damping, considering the power deposition profile and calculating the three dimensional ray tracing. The electron heating on the whole plasma region is observed at $\omega=2\omega_D$, and the heating is efficient and heating layer is localized by ion Bernstein wave in comparison with fast magnetosonic wave.

We would like to thank Dr. K. Ida for his help in calculating the ray tracing. This work was partly supported by a Grant-in-Aid for Scientific Research from the Japanese Ministry of Education.

References

1) I. B. Bernstein: Phys. Rev. Lett. **109** (1958) 10.
2) P. Lee, R. J. Taylor, W. A. Peebles, H. Park, C. X. Yu, Y. Xu, N. C. Luhmann, Jr., S. X. Jin: Phys.

Rev. Lett. **49** (1982) 205.

3) TFR Group, A. Truc, D. Gresillon: Nucl. Fusion **22** (1982) 1577.
4) K. Ida, M. Naito, S. Shinohara, K. Miyamoto: Nucl. Fusion **23** (1983) 1259.
5) K. Ida, O. Naito, I. Ochiai, S. Shinohara, K. Miyamoto: Nucl. Fusion **24** (1984) 375.
6) H. Park, N. C. Luhmann, Jr., W. A. Peebles, R. Kirkwood: Phys. Rev. Lett. **52** (1984) 1609.
7) M. Ono, K. L. Wong, G. A. Wurden: Phys. Fluids **26** (1983) 298.
8) M. Ono, G. A. Wurden, K. L. Wong: Phys. Rev. Lett. **52** (1984) 37.
9) K. Toi, T. Watari, K. Ohkubo, K. Kawahata, N. Noda *et al.*: *Proc. 10th Int. Conf. London, 1984* (Plasma Physics and Controlled Nuclear Fusion Research, 1984) (IAEA, Vienna, 1985) Vol. 1, p. 523.
10) M. Ono, T. Watari, R. Ando, J. Fujita, Y. Hirokura *et al.*: Phys. Rev. Lett. **54** (1985) 2239.
11) H. Abe, H. Okada, R. Itatani, M. Ono, H. Okuda: Phys. Rev. Lett. **53** (1984) 1153.
12) M. Porkolab: Phys. Rev. Lett. **54** (1985) 434.
13) K. Toi, S. Itoh, Y. Kawai, N. Hiraki, K. Nakamura, *et al.*: *Proc. 8th Int. Conf. Brussels, 1980* (Plasma Physics and Controlled Nuclear Fusion Research, 1980) (IAEA, Vienna, 1981) Vol. 1, p. 721.
14) S. Shinohara, K. Sakuma, Y. Nagayama, H. Toyama: J. Phys. Soc. Jpn. **52** (1983) 94.
15) S. Shinohara, N. Asakura, M. Naito, K. Miyamoto: J. Phys. Soc. Jpn. **53** (1984) 1746.
16) M. Ono, T. H. Stix, K. L. Wong, R. Horton: *Proc. the Second Joint Grenoble-Varenna Int. Symp. Heating in Toroidal Plasma* (1980) Vol. 1, p. 593.
17) A. Fukuyama, S. Nishizawa, K. Itoh, S. I. Itoh: Nucl. Fusion **23** (1983) 1005.